

# Tooth Root Bending Stress Distribution Characteristics of Gear in Wind Turbine Gear Transmission System

Wu Yang<sup>\*</sup>, Hou Li<sup>\*\*</sup>, Ma Dengqiu<sup>\*\*\*</sup>, Luo Lan<sup>\*\*\*\*</sup>  
and Wei Yongqiao<sup>\*\*\*\*\*</sup>

**Key words:** wind turbine gear transmission system; tooth root bending stress; distribution characteristics; deviation of gear clearance

## ABSTRACT

In this paper, distribution characteristics of tooth root bending stress of gear in wind turbine gear transmission are studied. Characteristics of wind speed in the long term and short term, the meshing characteristics and vibration status of single gear teeth are considered for more accurate results. A computing process for tooth root bending stress of gears in wind turbine gear transmission is put forward systematically. A sampling method is put forward by simplifying the relative displacement time series of gear drive to reduce computation load and improve efficiency according to Shannon Theorem and Gear Dynamics. And when the stress is calculated, single gear teeth are regarded as single elements of gear and their meshing processes are considered based on Gear Meshing Theory. At last, the probability density curve of tooth root bending stress of sun gear is derived. Changes of distribution characteristics of tooth root bending stress of sun gear with deviation of gear clearance are discussed at two damping levels.

*Paper Received May, 2019. Revised November, 2019. Accepted December, 2019. Author for Correspondence: Hou Li.*

*\* Doctoral Student, School of Mechanical Engineering, Sichuan Univ., Chengdu, 610065, China*

*\*\* Professor, School of Mechanical Engineering, Sichuan Univ., Chengdu, 610065, China*

*\*\*\* Doctoral Student, College of Eng. and Technol., Zunyi Normal College, Zunyi 563006, China*

*\*\*\*\* Doctoral Student, School of Mechanical Engineering, Sichuan Univ., Chengdu 610065, China*

*\*\*\*\*\* Associate Professor, School of Mechatronics Eng., Lanzhou Univ. of Technol., Lanzhou 730050, China*

## INTRODUCTION

Gear tooth root bending fatigue failure is one of the main failure forms of wind turbine transmission system [Sheng et al., 2011]. In order to avoid premature failure of wind turbine transmission system due to tooth root bending fatigue failure, it is essential to make clear distribution characteristics of tooth root bending stress of gears in the system. However, only few research was conducted in this field. Nejad et al. [2014] studied the short term and long term probability density functions of gear tooth root bending stress of a 5MW wind turbine gear transmission system based on multibody simulation method and ISO 6336-6. But the actual meshing process of single teeth was ignored which would lead to inaccurate distribution functions. Martin F.J. et al. [2014] calculated tooth root bending stress of gears based on multibody simulation method and FEM for a 500 kW wind turbine. And the actual meshing process of single teeth were considered. But the distribution characteristics of tooth root bending stress were not studied. Qiu Y. et al. [2017] researched influences of turbulence intensity on characteristics of gear tooth root bending stress distributions. But the actual meshing process of single teeth was still not considered.

The distribution analysis of tooth root bending stress of the system is a multidisciplinary problem, in which Aerodynamics, Gear Dynamics, Gear Meshing Principle, Material Mechanics and Probability Theory are involved. In the long term, the mean wind speed obeys a certain distribution form, such as Weibull Distribution, or Rayleigh Distribution [He D., 2006]. And the short term wind speed consists of average wind speed and turbulent wind speed. The turbulent part is considered as a stochastic process in engineering [He D., 2006]. Random Phase Harmonic Superposition Method, Autoregressive (AR) Method and Autoregressive moving-average (ARMA) Method were put forward

to simulate the turbulent wind speed[Wang Y.,2008]. For the dynamic modeling of the system, several models were applied, such as Finite Element Model[Zhao Y. et al. ,2014; Wang S. et al.,2017; Kim S.W. et al.,2017], Multibody Model[Dong W. et al.,2012; Bruce T. et al.,2015; Jorgensen M.F. et al.,2014; Li H. & Cho H.,2017] and Lumped Mass Parameter Model[Qiu Y. et al.,2017; Yang J. & Zhang L.P.,2011; Gui Y. et al.,2014; Zhai H. & Zhu C.,2015; Zhao M. & Ji J.C.,2015; Gallego-Calderon J. & Natarajan A. ,2015] and so on. Finite element Model has the highest accuracy but the longest calculation time and is difficult to converge when the model is too complex or the simulation process is too long. The accuracy of Multibody Model and Lumped Mass Parameter Model meet requirements of industrial applications with reasonable parameter settings and are easy to converge with much less calculation time and smaller computation load than Finite Element Model. So these two models are more widely used to analyze the dynamic characteristics of the system. As single gear teeth are basic elements to transfer load and motion, the failure of a gear is actually the failure of single gear teeth on the gear. So when stress is calculated, the actual meshing process and vibration status of single gear teeth must be considered. Usually, the calculated cyclic stress is an asymmetric one which is not available for reliability design and life evaluation directly. Goodman Model and Gerber Model are widely used to convert asymmetrical cyclic stress to symmetrical cyclic stress in engineering[GOODMAN J.,1941; GERBER W.Z.,1874]. While Gerber Model is more applicable for plastic materials, Goodman Model is more suitable for brittle materials[Liu X. & LIU G.,2018]. But considering that Goodman Model is simpler, safer and more conservative than Gerber model, it is more widely used in design stage of structural components. For the stress distribution analysis, Rain Flow Counting Algorithm is widely used to simplify the measured load history into load cycles in industrial applications[NIESŁONY A.,2009].

In this paper, distribution characteristics of gear tooth root bending stress of the system are studied. In the long term, mean wind speed is described by Weibull Distribution. And in the short term, instantaneous wind speed is simulated with AR Method. The dynamic model of the system is established based on Lumped Mass Parameter Method. The influences of parameter varying with wind speed on the dynamic response are concerned. And before computing tooth root bending stress, the relative displacement time series between gear teeth are simplified by a sampling method. In this method, a single gear tooth is regarded as an element. Its actual meshing process and vibration status are considered with Gear Meshing Theory and Gear Dynamics. Then tooth root bending stress of each

single gear tooth is calculated. Goodman Model is applied to transfer the asymmetrical stress cycle to symmetrical one. Tooth root bending stress distribution curves in the short term are derived by Rain Flow Counting Algorithm. Later, the distribution curve of tooth root bending stress in the long term is obtained by a weighted summation of distribution curves in the short term. Finally, tooth root bending stress distribution characteristics of sun gear are studied. The influences of gear clearances on distribution characteristics are also discussed with two damping levels.

## MODELING OF WIND SPEED

The instantaneous wind speed in a wind field can be expressed as follows[He D.,2006]:

$$V(t) = \bar{V}(t) + V'(t) \quad (1)$$

Though  $\bar{V}$  changes randomly over time, its distribution conforms to a certain statistical law. In this paper, Weibull Distribution is applied to

describe the long-term distribution of  $\bar{V}$ . The probability density function of Weibull Distribution are [He D.,2006]:

$$f(\bar{V}) = \frac{\kappa}{\zeta} \left(\frac{\bar{V}}{\zeta}\right)^{\kappa-1} \exp\left[-\left(\frac{\bar{V}}{\zeta}\right)^\kappa\right] \quad (2)$$

$V'$  changes with amplitudes related to  $\bar{V}$ . And in engineering, the changing process of  $V'$  can be regarded as a stochastic process and can usually be described by the turbulence power spectrum in a neutrally stable atmosphere[Chen H. et al.,2017]. In this paper, AR Method is applied to simulate the stochastic process based on Von Karman Spectrum. The AR model can be expressed as follows[Van D.H.E.L. et al.,2003]:

$$V'(t) = \sum_{k=1}^p \psi_k V'(t - k\Delta t) + \sigma_N N(t) \quad (3)$$

where  $N(t)$  is an independent stochastic process with mean value of 0 and variance of 1,  $\sigma_N$  is the standard deviation of wind speed time series, and  $\sigma_N N(t)$  is the random error.

According to Wiener-Khinchin Formula, the autocorrelation function can be derived as follows:

$$R(\tau) = \int_0^\infty S(\omega) e^{i\omega\tau} d\omega \quad (4)$$

where  $S(\omega)$  is Von Karman Spectrum.

Von Karman Spectrum can be expressed as follows:

$$S(\omega) = \frac{4\sigma^2 l / \bar{V}}{(1 + 71(\omega l / \bar{V})^2)^{\frac{5}{6}}} \quad (5)$$

With Equations (3)-(5),  $V'(t)$  can be achieved by calculating  $\psi_k$  and  $\sigma_N$ . Then  $c$  with a certain  $\bar{V}$  can be obtained.

In order to take into the influences of long term and short term wind speed characteristics on stress distribution characteristics, we disperse the long-term probability density function of mean wind speed into parts with a width of 2m/s equally. And the wind speed model of each part is simulated by AR Method as shown in Figure 1.

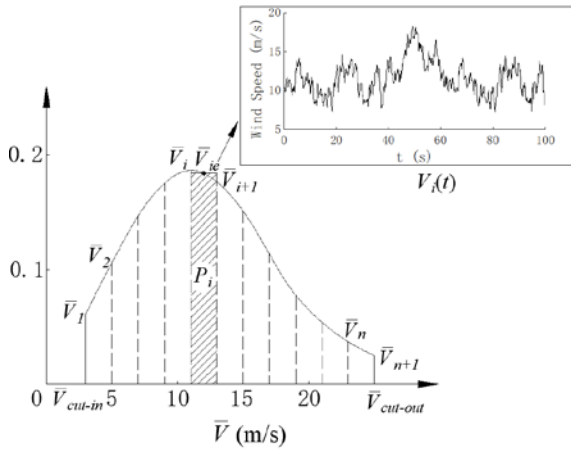


Fig. 1 Wind speed modeling

According to Aerodynamics Theory of Wind Turbine, the input power can be calculated as follows [Yang J., 2012].

$$P_{in} = \frac{1}{2} \rho \pi r^2 V^3(t) C_p \quad (6)$$

The input torque and output torque are [Yang J., 2012]:

$$T_{in} = \frac{P_{in}}{\omega_c} \quad (7)$$

$$T_{out} = \frac{T_{in}}{i_s} \quad (8)$$

## DYNAMIC MODELING OF THE SYSTEM

The wind turbine gear transmission system consists of a planetary gear drive and a two stage fixed axis gear transmission. Based on lumped-mass method [ZHANG C., 2012], the torsional dynamic model of system is built as shown in Figure 2.

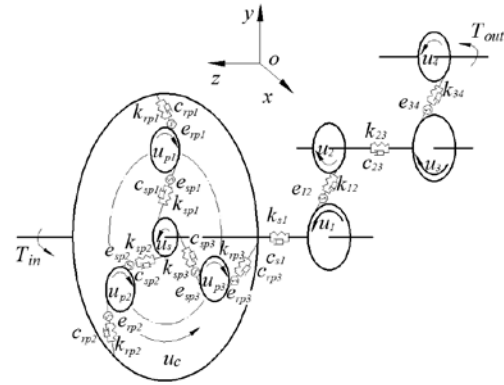


Fig. 2 Torsional dynamic model of the system

Displacements between components without considering meshing errors are defined as follows:

$$\begin{cases} \Delta_{rpj} = u_c \cos \alpha_{rp} - u_{pj} \\ \Delta_{spj} = u_{pj} + u_c \cos \alpha_{sp} - u_s \\ \Delta_{12} = u_1 - u_2 \\ \Delta_{34} = u_3 - u_4 \\ \Delta_{s1} = \frac{u_s}{r_s} - \frac{u_1}{r_1} \\ \Delta_{23} = \frac{u_2}{r_2} - \frac{u_3}{r_3} \end{cases} \quad (9)$$

According to Equation (9), there exist relationships between  $\Delta_{spj}$  and  $\Delta_{rpj}$  :

$$\begin{cases} \Delta_{sp2} = \Delta_{sp1} + \Delta_{rp1} - \Delta_{rp2} \\ \Delta_{sp3} = \Delta_{sp1} + \Delta_{rp1} - \Delta_{rp3} \end{cases} \quad (10)$$

So only eight independent parameters are needed to describe the vibration of the system. Here,  $\Delta_{sp1}, \Delta_{rp1}, \Delta_{rp2}, \Delta_{rp3}, \Delta_{s1}, \Delta_{12}, \Delta_{23}, \Delta_{34}$  are chosen as independent parameters. Based on Newton's Second Law and liner transform of matrix, the dynamic function of the system with positive definite stiffness matrix can be derived:

$$\mathbf{M}\Delta'' + \mathbf{c}\Delta' + \mathbf{Kf}(\Delta) = \mathbf{F}_{in} + \mathbf{F}_{ex} \quad (11)$$

where  $\mathbf{f}(\ast)$  is the clearance function.

Considering that the mean value of  $V_i(t)$  is  $V_{ie}$ , a simplify is done here: dynamic parameters corresponding to  $V_i(t)$  is assumed to be equal to dynamic parameters corresponding to  $V_{ie}$  except the torque.

## CALCULATING OF TOOTH ROOT BENDING STRESS PROBABILITY DENSITY CURVE

### Sampling of Relative Displacement Time Series of Gear Drive

With Runge-Kutta Method, the relative displacement time series of different DOFs can be obtained by solving Equation (11). However, because main features of relative displacement time series can be described by peaks and bottoms, the time series are redundant as shown in Figure. 3. And with the bottoms and peaks in the time series, the main features of stress time series of gear can be derived with further computation. In order to simplify the time series for less calculating time, a sampling method is proposed based on Shannon Theorem [Shannon C.E.J,1949] and Mode Superposition Method[ZHANG C.,2012]. According to Shannon Theorem, in order to restore the signal with distortion, the sampling frequency should be at least twice as high as the highest frequency in the spectrum of the signal.

$$\omega_s \geq 2\omega_{\max} \quad (12)$$

And according to Mode Superposition Method, displacements of Eq.(11) are superposition of all modes.

$$\Delta(t) = \sum \eta_i(t)\phi^{(i)} \quad (13)$$

$$\eta_i(t) = \frac{1}{\omega_{di}} \int_0^t N_i(\tau) e^{-\xi_i \omega_i(t-\tau)} \sin \omega_{di}(t-\tau) d\tau \quad (14)$$

According to Equations (13) and (14), the highest frequency in the spectrum of displacement is the maximal  $\omega_{di}$ . And the damping natural frequency is slightly smaller than the undamped one. In order to simplifying computation of  $\omega_{\max}$ , the damping is ignored.

$$\omega_{\max} = \left\{ \omega \mid \left| \mathbf{K} - \omega^2 \mathbf{M} \right| = \mathbf{0} \right\}_{\max} \quad (15)$$

The sampling period is derived as follows:

$$T_s = \frac{2\pi}{n_\omega \omega_{\max}} \quad (16)$$

With the sampling method, the data size can be reduced obviously as shown in Figure 4.

As single gear teeth are basic elements to transfer load and motion, the displacement of each single gear tooth should be obtained first for further analysis. A single gear tooth meshes once when the gear rotates a single revolution. According to Gear Meshing Theory, the meshing period of a gear is:

$$T_m = \frac{2\pi}{\omega_g z_g} \quad (17)$$

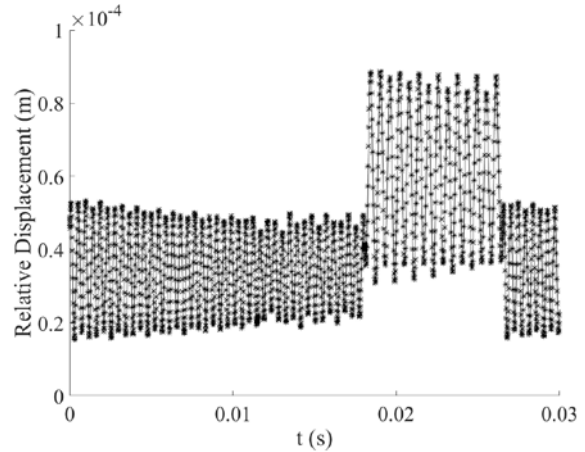


Fig. 3 Unsamped Relative Displacement Time Series

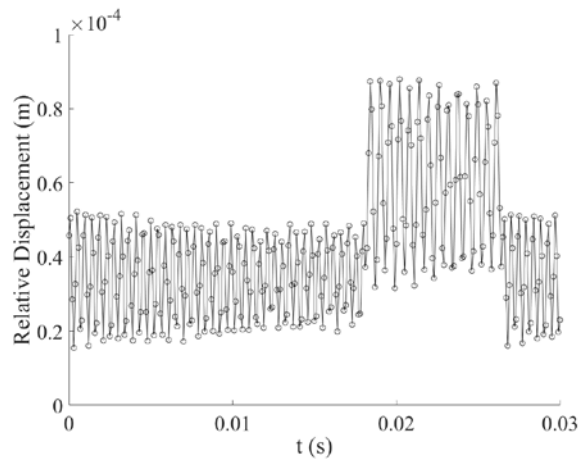


Fig.4 Sampled Relative Displacement Time Series( $n_\omega=8$ )

And the meshing time for a single gear tooth is  $(1 + \varepsilon)T_m$ , so the number of sampling points for a single tooth on the desired gear can be derived.

$$n_t = \frac{(1 + \varepsilon)T_m}{T_s} \quad (18)$$

Generally, enough relative displacement time series data is needed to calculate tooth root bending stress of a single gear tooth. However, its computing costs would be too high. For example if we want to get 100s long relative displacement time series data for a single tooth on a gear with 27 teeth, 2700s long relative displacement time series data of the gear drive is required. In order to reduce computing cost, it is assumed that relative displacement time series of a single gear tooth are sums of relative displacement time series of all gear teeth on the gear. The assumption is reasonable, because a single gear tooth would meet all the input torque cases and the input torque cases of different single gear teeth are the same in the sense of probability during the life

time of the system

The time ranges when different teeth are in mesh are derived based on Gear Meshing Theory [Sun H., 1996].

$$\begin{cases} t_s = (1 - \gamma)T_m + nT_m \\ t_e = (2 + \varepsilon - \gamma)T_m + nT_m \end{cases} \quad n = 0, 1, 2, \dots, K \quad (19)$$

With Equation (19), the relative displacement time series of a single tooth can be cut into relative displacement time series of different single teeth as shown in Figure 5.

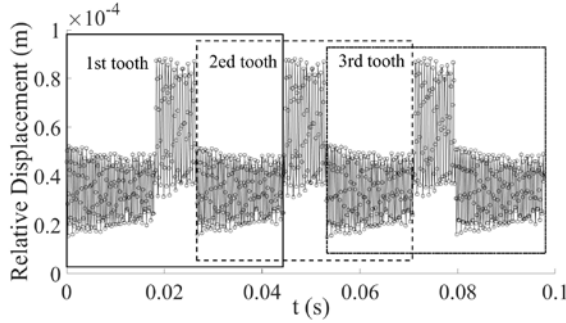


Fig. 5 Relative Displacement Time Series of a single tooth

With the relative displacement time series of a single tooth, its meshing force time series can be obtained. For the point  $q$  in a meshing period, the meshing force is:

$$F_q = K_{\alpha q} k_q \delta_q \quad (20)$$

$$K_{\alpha q} = \frac{k_{q1}}{k_{q1} + k_{q2}} \quad (21)$$

According to characteristics of involutes [Sun H., 1996], the pressure angle is:

$$\alpha_q = \begin{cases} \tan^{-1}(\tan \alpha_f \pm \phi_q) & \text{the driving gear} \\ \tan^{-1}(\tan \alpha_f \mp \phi_q) & \text{the driven gear} \end{cases} \quad (22)$$

where if the gear is an external gear, the “+” will be chosen from “ $\pm$ ”, otherwise the “-” will be chosen

With Equation (22), the tooth root bending stress can be calculated [ISO 6336-3:2006].

$$\sigma_{qF} = Y_{Fq} Y_{Sq} \frac{F_q}{Bm} \quad (23)$$

### Probability Density Function of Tooth Root Bending Stress

With steps above, tooth root bending stress time series of a single tooth can be achieved. And then with Rain-flow Counting Algorithm and Goodman Model, probability density functions of tooth root bending stress of a single gear tooth for different short term wind speed models can be

achieved.

Table 1 Rain-flow Counting Algorithm flow

<b>Step 1:</b> Input the load time series.
<b>Step 2:</b> Read next peak or valley. If out of data, go to Step 7.
<b>Step 3:</b> If there are less than three points, go to Step 2. Form ranges $X$ and $Y$ using the three most recent peaks and valleys that have not been discarded.
<b>Step 4:</b> Compare the absolute values of ranges $X$ and $Y$ . If $X < Y$ , go to Step 2. If $X \geq Y$ , go to Step 5.
<b>Step 5:</b> If range $Y$ contains the starting point $S$ , go to Step 6; otherwise, count range $Y$ as one cycle; discard the peak and valley of $Y$ ; and go to Step 3.
<b>Step 6:</b> Count range $Y$ as one-half cycle; discard the first point (peak or valley) in range $Y$ , move the starting point to the second point in range $Y$ ; and go to Step 3.
<b>Step 7:</b> Count each range that has not been previously counted as one-half cycle.

Rain-flow Counting Algorithm is an algorithm to simplify the measured load history into several load cycles for fatigue analysis. In this algorithm, the amplitude and the mean value of load cycle are considered, which are in accordance with the inherent characteristics of fatigue load. Let  $S$  denote starting point in the load time series;  $S_1$ , point next to  $S$ ;  $S_2$ , point next to  $S_1$ ;  $X$ , range under consideration,  $X = |S_1 - S_2|$ ;  $Y$ , previous range adjacent to  $X$ ,  $Y = |S - S_1|$ . The Rain-flow Counting Algorithm flow is shown in Table 1 [ASTM E1049-85(2017)].

According to Goodman Model, the amplitude of asymmetrical cyclic stress can be transferred to amplitude of symmetrical cyclic stress [GOODMAN J., 1941].

$$\sigma_{as} = \frac{\sigma_{aa}}{1 - (\sigma_m / \sigma_b)} \quad (24)$$

According to the symmetrical cyclic stress time series, the approximate short term probability density function of tooth root bending stress of a single tooth can be obtained.

$$f_s^i(\sigma_{as}) = \frac{C^i(\sigma_{as})}{C_{total}^i} \quad (25)$$

where  $C^i(\sigma_{as})$  is the counting times of  $\sigma_{as}$  for the  $i$ th short term wind speed.

The approximate long term probability density function is derived.

$$f_l(\sigma_{as}) = \frac{\sum_{i=1}^n N_i C^i(\sigma_{as})}{\sum_{i=1}^n N_i C_{total}^i} \quad (26)$$

Above all, a computing process to get tooth root bending distribution characteristics for wind turbine gear transmission system is put forward. Applying the computing process, the tooth root

bending distribution characteristics, such as equivalent symmetric cyclic stress, number of stress cycles, stress distribution rule, can be derived. And with the stress characteristics, further analysis and design for wind turbine gear transmission system, such as fatigue life estimation, structural parameter optimization can be conducted. The simplified computing process are concluded in Table 2.

Table 2 Computing process of tooth root bending stress probability density function of wind turbine gear transmission system

**Step 1:** Determine technical parameters of the wind turbine and geometric parameters of the gear transmission system. Chose a target gear.

**Step 2:** Determine Weibull Distribution  $f(V)$  of the wind field. Simulate short-term wind speed models  $V_1(t), V_2(t), \dots, V_n(t)$ .

**Step 3:** When  $i \leq n$ , calculate the cycle counts and short-term probability density function  $f_s^i(\sigma_{as})$  of tooth root bending stress for the target gear under  $V_i(t)$ .

**Step 4:** Based on the cycle counts of tooth root bending stress of target gear under  $V_1(t), V_2(t), \dots, V_n(t)$ , calculate the long-term probability density function  $f_l(\sigma_{as})$  of tooth root bending stress of the target gear.

**EXAMPLES**

In this paper, we study distribution characteristics of tooth root bending stress of sun gear. The technical parameters of the wind turbine are given in Table 3, Figure. 6 and Figure. 7. The geometric parameters of the wind turbine gear transmission system are shown in Table 4.

Table 3 Technical Parameters

Item	Value
Rated power (MW)	1.5
Impeller radius (m)	34
Design rotational speed (rpm)	19.35
Rated wind speed (m/s)	11.3
Air density (kg/m <sup>3</sup> )	1.21
Cut-in wind speed(m/s)	3
Cut-off wind speed(m/s)	20
mean wind speed (m/s)	11.3
turbulence coefficient	0.2
variance of mean wind speed (m <sup>2</sup> /s <sup>2</sup> )	9
material of gear	20CrMnTi

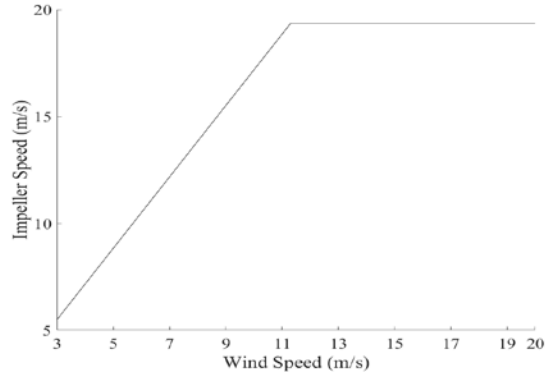


Fig. 6 The impeller speed curve

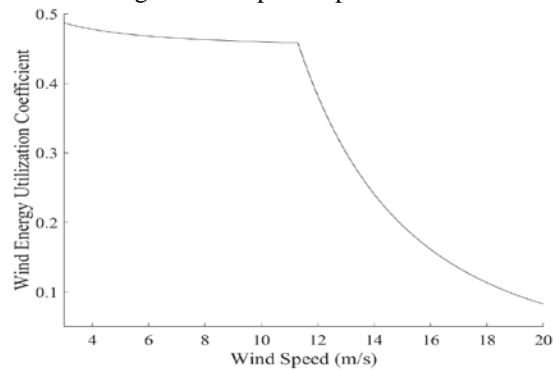


Fig. 7 The wind energy utilization curve

Table 4 Geometric parameters of the wind turbine transmission system

Stage	Item	Sun gear	Ring gear	Planet gear
1st	Number of teeth	27	117	44
	Pressure angle(°)	20		
	Tooth width(mm)	370		
	Normal module(mm)	13		
	gear clearance(um)	260		
	Amplitude of $e_{rpi}$ (um)	68		
2nd	Amplitude of $e_{spi}$ (um)	64		
	Item	Gear 1	Gear 2	
	Number of teeth	104	23	
	Pressure angle(°)	20		
	Tooth width(mm)	350		
	Normal module(mm)	10		
3rd	gear clearance(um)	340		
	Amplitude of $e_{l2}$ (um)	69		
	Item	Gear 3	Gear 4	
	Number of teeth	98	25	
	Pressure angle(°)	20		
	Tooth width(mm)	6.5		
3rd	Normal module(mm)	20		
	gear clearance(um)	260		
	Amplitude of $e_{34}$ (um)	60		

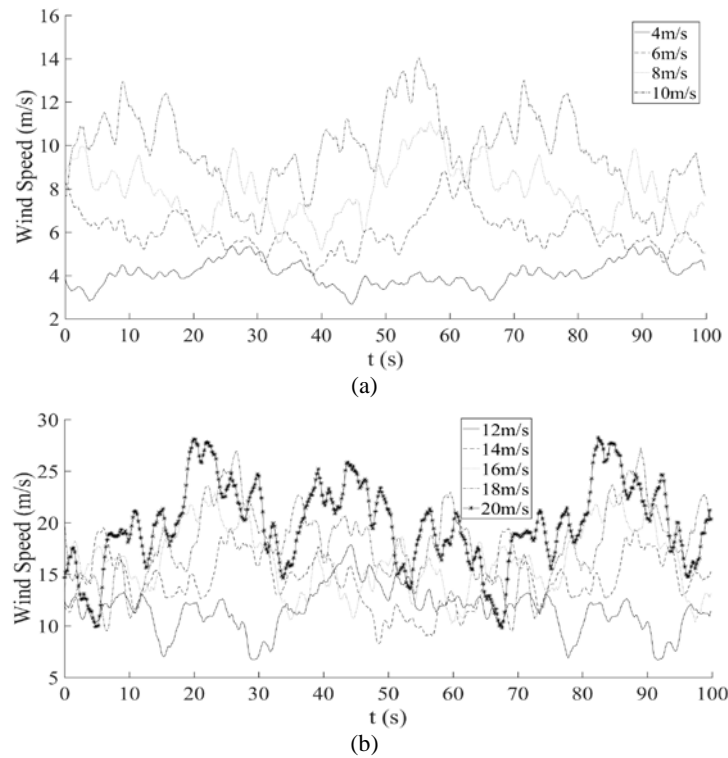


Fig. 8 Short term wind speed models

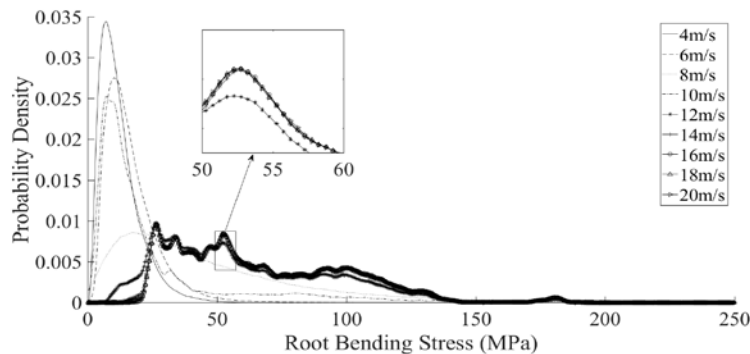


Fig. 9 Probability density curves of tooth root bending stress of sun gear for different short term wind speed models with no gear clearance deviation (damping factor equals to 0.03)

With parameters of the wind field, short term wind speed models with different mean wind speeds are obtained by the AR Model as shown in Figure 8.

**Distribution Characteristics of Tooth Root Bending Stress of Sun Gear with No Gear Clearance Deviation when Damping Factor Equals to 0.03**

Based on short term wind speed models, dynamic parameters of the system are achieved with Equations (6-8) and Fig. 6, Fig. 7. With dynamic parameters of the system, relative displacement time series of sun gear is achieved by solving Eq.

(11) for different short term wind speed models. And with the sampling method, sampled relative displacement time series of a single gear tooth for sun gear can be obtained. Then with Equations (17-24), the symmetrical cyclic stress time series of sun gear for different short term wind speed models are obtained. And by means of Rain Flow Counting Algorithm and Equation (25), probability density curves of tooth root bending stress of sun gear for different short term wind speed models can be achieved as shown in Figure 9. And then according to Equation (26), the probability density curve of root bending stress of sun gear in the long term are derived as shown in Figure 10.

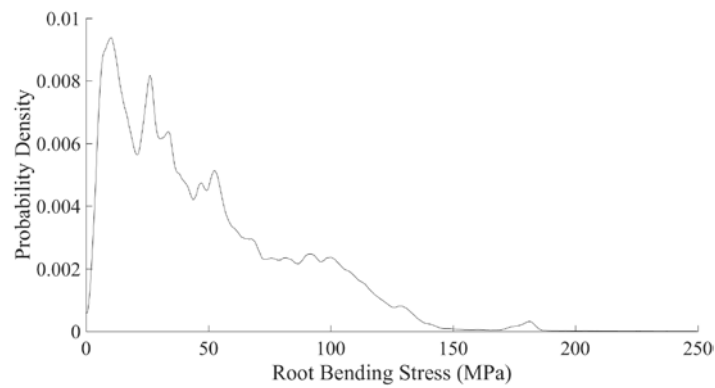


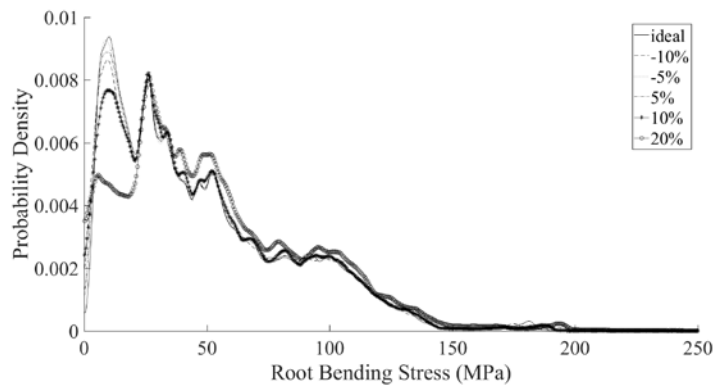
Fig. 10 Probability density curve of root bending stress of sun gear in the long term with no gear clearance deviation (damping factor equals to 0.03)

In Fig. 9, distribution forms are nearly the same when mean wind speed is smaller than rated wind speed except the positions of peak are different. The main reason is that the short wind speed is in the range of 3m/s to 11.3m/s for those short term wind speed models. Thus, according to Fig. 7, the distribution forms of input torque are approximate to those of wind speed models which are nearly fitted by normal distribution. And the system is weakly nonlinear, so the input(input torque) is transferred to the output(stress) nearly linearly. When mean wind speed is larger than rated speed, probability density curves are also nearly the same. It is because that the distribution curve of valid input torque of each short term wind speed model is similar to each other with rated input torques all taking up a large part in gross torques. From Fig. 10, it can be known that the long term distribution of tooth root bending stress of sun gear does not conform to any distribution form. Thus a fitting function is more suitable to describe the probability density curve. While the low stress part of the curve is mainly determined by short term wind speed models with mean wind speed smaller than rated wind speed, the medium and high stress parts

are mainly influenced by short term wind speed models with mean wind speed larger than rated wind speed.

**Effect of Gear Clearance Deviations on Distribution Characteristics of Tooth Root Bending Stress of Sun Gear in The Long Term when Damping Factor Equals to 0.03**

Considering manufacturing errors and assembly errors, gear clearances deviates from the design values. For robust design of the system, it is important to know how the deviation of gear clearances influence the distribution of tooth root bending stress of gears. In this part, the influences of deviations of gear clearances between sun gear and planet gear 1 and between ring gear and planet gear 1 on the long term distribution of tooth root bending stress of sun gear are studied. The deviations are -10%, -5%, 5%, 10% and 20% of the design value respectively. Figure 11 and Figure 12 show the influence of deviations of gear clearances on the long term distribution of tooth root bending stress of sun gear.



(a) Probability density curves

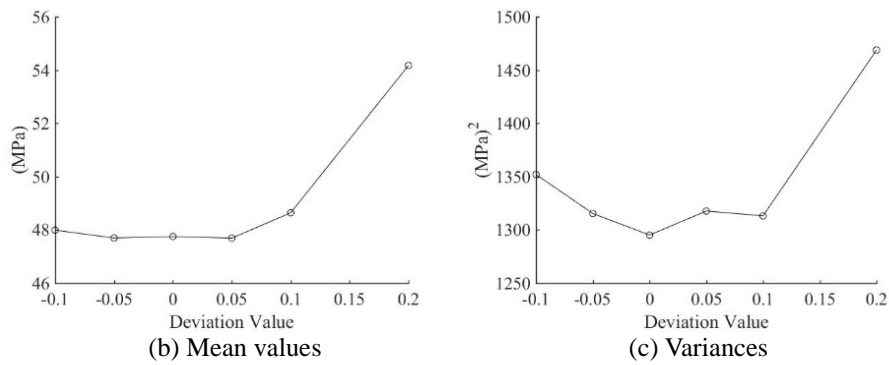


Fig. 11 Distribution characteristics of tooth root bending stress of sun gear in the long term with different gear clearances deviations between sun gear and planet gear 1(damping factor equals to 0.03)

From Fig. 11(a), it is known that the deviations all lead to decrease of the proportion of low stress and increase of the proportion of medium and high stress. With the increase of deviation, this trend intensifies gradually. When absolute values of deviations are equal, the influence of positive ones is larger than that of the negative ones. And when the deviation is 20%, the distribution form is changed significantly which may shorten the

working life of the transmission system. From Fig.11(b) and (c), we can find that the deviation causes the increase of mean value and variance of stress distribution. And with the increase of deviation in positive and negative directions, both the mean value and variance increase nonlinearly. The varying curve is similar to that of a concave function, and the slope becomes larger when the deviation increases.

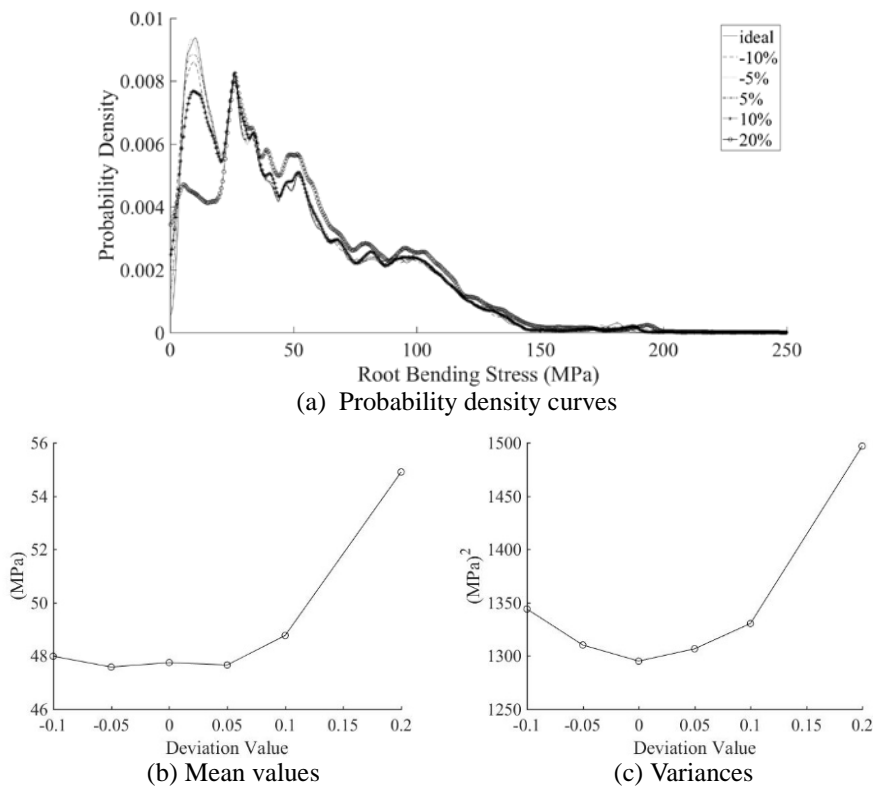


Fig. 12 Distribution characteristics of tooth root bending stress of sun gear in the long term with different gear clearances deviations between ring gear and planet gear 1(damping factor equals to 0.03)

From Fig. 12, we can find that the influences of gear clearances deviations between ring gear and planet gear 1 on the stress distribution

characteristics of sun gear are nearly the same with those of deviations of gear clearances between sun gear and planet gear 1.

**Distribution Characteristics of Tooth Root Bending Stress of Sun Gear in The Long Term with Large Damping**

In this instance, the influence of deviation of gear clearance between sun gear and planet gear 1

on the long term distribution characteristics of tooth root bending stress of sun gear with large damping is studied. Here the damping factor is 0.17. The deviations are also -10%, -5%, 5%, 10% and 20% of the design value respectively. The results are shown in Figure 13.

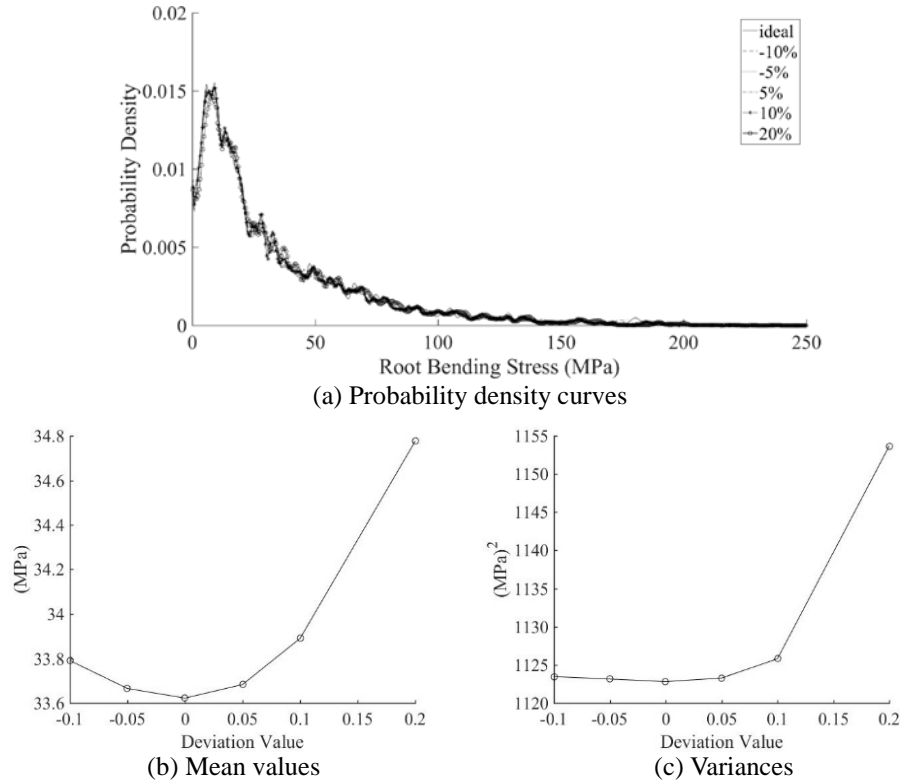


Fig. 13 Distribution characteristics of tooth root bending stress of sun gear in the long term with different deviations of gear clearance between sun gear and planet gear 1(damping factor equals to 0.17)

By comparing Fig. 10 with Fig. 13(a), it is known that the distribution form with large damping is quite different from that with small damping. The low stress part of the former takes up much larger portion and the curve of the former is more smooth without big fluctuates. And the mean value and variance of the former are much smaller than those of the latter ones. Fig. 13(a) shows that the influence of gear clearance deviations is very small on the stress distribution forms. The curves almost coincide. From Fig. 13(b) and (c), we can find that mean values and variances all increase with enlarging of deviation in positive and negative directions nonlinearly. But the increase is very small. So it can be concluded that a large damping factor greatly reduces the sensitivity of stress distribution characteristics to gear clearance deviations

**CONCLUSIONS**

A computing process is put forward to calculate probability density function of tooth root

bending stress for wind turbine gear transmission system. A sampling method is put forward to reduce the data size of relative displacement time series for less computing time. In the process, characteristics of wind speed in the long term and short term, the meshing characteristics and vibration status of single gear teeth are considered for more accurate results.

With the computing process, the tooth root bending stress distribution characteristics of sun gear in different situations are studied. Several valuable conclusions are obtained. Firstly, the distribution of tooth root bending stress in the long term does not conform to any probability distribution form. Secondly, gear clearance deviations will lead to decrease of the proportion of low stress part and increase of the proportion of medium and high stress parts. And this change is more significant with larger clearance deviation. Lastly, the varying of damping factor will lead to change of long term distribution form of tooth root bending stress of sun gear significantly. Large damping greatly reduces the sensitivity of tooth root

bending stress distribution characteristics to gear clearance deviation.

## FUNDINGS

This research is supported by National Natural Science Foundation of China (Grant No. 51375320), Natural Science Foundation of Gansu Province (Grant No. 18JR3RA140), Natural Science Foundation of Education Department of Guizhou Province(Grant No. QianjiaoheKYzi[2018]319Hao).

## REFERENCES

- ASTM E1049-85(2017), Standard Practices for Cycle Counting in Fatigue Analysis, 2017.
- Bruce T., Long H., Dwyer-Joyce R., "Dynamic modelling of wind turbine gearbox bearing loading during transient events," *IET Enewable Power Generation*, Vol.9, No.7, pp.821-830, (2015).
- Chen H., Wang X., Gao H., "Dynamic Characteristics of Wind Turbine Gear Transmission System with Random Wind and The Effect of Random Backlash on System Stability," *Archive Proceedings of the Institution of Mechanical Engineers Part C: Journal of Mechanical Engineering Science*, Vol.231, No.14, pp.590-2597, (2017).
- Dong W., Xing., "Time Domain Modeling and Analysis of Dynamic Gear, Contact Force in a Wind Turbine Gearbox with Respect to Fatigue Assessment," *Energies*, Vol.5, No.11, pp.4350-4371, (2012).
- Gallego-Calderon J., Natarajan A., "Assessment of wind turbine drive-train fatigue loads under torsional excitation," *Engineering Structures*, Vol.103, pp.189-202, (2015).
- GERBER W.Z., "Investigation of the allowable stress in iron construction," *Bayer Arch. Ing. Ver.* Vol.6, No.6, pp.101-110 (1874).
- GOODMAN J., *Mechanics applied to engineering*. Longmans, London, (1941).
- Gui Y., Han Q.K., Li Z., "Detection and Localization of Tooth Breakage Fault on Wind Turbine Planetary Gear System considering Gear Manufacturing Errors," *Shock and Vibration*, Vol.2014, pp.1-13, (2014).
- He D., *Wind Engineering and Industrial Aerodynamics*, National Defense Industry Press, Beijing (2006).
- ISO 6336-3:2006, Calculation of load capacity of spur and helical gears, (2006).
- Jorgensen M.F., Pedersen N.L., Sorensen J.N., Paulsen U.S. "Rigid MATLAB drivetrain model of a 500 kW wind turbine for predicting maximum gear tooth stresses in a planetary gearbox using multibody gear constraints," *Wind Energy*, Vol.17, No.11, pp.1659-1676, (2014).
- Kim S.W., Lee Y.S. Jang D.W., "Fatigue life evaluation of pinion gears for the reliability of pitch systems in wind turbines," *Journal of Mechanical Science and Technology*, Vol.31, No.2, pp.753-758, (2017).
- Li H., Cho H., Sugiyama H., "Reliability-based design optimization of wind turbine drivetrain with integrated multibody gear dynamics simulation considering wind load uncertainty," *Structural and Multidisciplinary Optimization*, Vol.56, No.1, pp.183-201, (2017).
- Liu X., LIU G., "Study on fatigue life prediction of Q345 steel under stress control," *Journal of Plasticity Engineering*, Vol.3, No.25, pp.212-216, (2018).
- Martin F.J., N.L. P., Jens N.S., "Gear fatigue damage for a 500 kW wind turbine exposed to increasing turbulence using a flexible multibody model," *Modeling Identification & Control*, Vol.35, No.2, pp.109-125, (2014).
- Nejad, Amir R., Z. G., T. M., "On long-term fatigue damage and reliability analysis of gears under wind loads in offshore wind turbine drivetrains," *International Journal of Fatigue*, Vol.61, pp.116-128, (2014).
- NIESŁONY A., "Determination of fragments of multiaxial service loading strongly influencing the fatigue of machine components," *Mechanical Systems and Signal Processing*, Vol.23, No.8, pp.2712-2721, (2009).
- Qiu Y., Chen L., Feng, Y., X Y., "An Approach of Quantifying Gear Fatigue Life for Wind Turbine Gearboxes Using Supervisory Control and Data Acquisition Data," *ENERGIES*, Vol.10, No.8, pp.1084, (2017).
- Shannon C.E., "Communication in the presence of noise," *Proc. IRE*, Vol.37, pp.10-21, (1949).
- Sheng, McDade, Errichello. "Wind Turbine Gearbox Failure Modes-A Brief (Presentation)," *Office of Scientific & Technical Information Technical Reports*, (2011).
- Sun H., *Mechanical Principle*, Higher Education Press, Beijing, (1996).
- Van D.H.E.L., Schaak P., Van E.T.G., "Wind turbine control algorithms," *Energy Research*

Centre of the Netherlands, Netherlands(2003).

Wang S., Zhu C., Song C., “Effects of gear modifications on the dynamic characteristics of wind turbine gearbox considering elastic support of the gearbox,” Journal of Mechanical Science and Technology, Vol.31, No.3, pp.1079-1088,(2017).

Wang Y., SUN C., LI X.. “Short-term Wind Speed Simulation Corrected With Field Measured Wind Speed,” Proceedings of the CSEE, Vol.28, No.11, pp.94-100,(2008).

Yang J., Zhang L.P., “Dynamic Response and Dynamic Load of Wind Turbine Planetary Gear Transmission System Under Changing Excitation,” Applied Mechanics and Materials, Vol.121-126, pp.2671-2675,(2011).

Yang J., “Study on Dynamics Characteristics of Planetary Gear Transmission System of Wind Turbine under Varying Loads,” Ph. D. Thesis, Chongqing University, Chongqing, China(2012).

ZHANG C., Mechanical Dynamics (Second Edition) , Higher Education Press ,Beijing, ( 2012).

Zhai H., Zhu C., Song C., “ Dynamic modeling and analysis for transmission system of high-power wind turbine gearbox,” Journal of Mechanical Science & Technology, Vol. 29, No.10, pp.4073-4082,(2015).

Zhao M., Ji J.C., “Nonlinear torsional vibrations of a wind turbine gearbox,” Applied Mathematical Modelling,” Vol.39, No.16, pp.4928-4950,(2015).

Zhao Y., Ahmat M., Bari K., “Nonlinear dynamics modeling and analysis of transmission error of wind turbine planetary gear system,” Proceedings of the Institution of Mechanical Engineers Part K-Journal of Multi-body Dynamics, Vol.228, No.4, pp.438-448,(2014).

### NOMENCLATURE

$B$  tooth width

$C_p$  wind power coefficient

$c_{rpi}$  mesh damping of ring gear and planet gear  $j$

$c_{spj}$  mesh damping of sun gear and planet gear  $j$

$c_{12}$  mesh damping of gear 1 and gear 2

$c_{34}$  mean mesh damping of gear 3 and gear 4

$c_{s1}$  torsional damping of connecting shafts between sun gear and gear 1

torsional damping of connecting shafts between gear 2 and gear 3

$\mathbf{c}$  damping matrix

total counting times of stress cycle for the  $i$  th short term wind speed model

$e_{rpi}$  transmission errors of ring gear and planet gear  $j$

$e_{spj}$  transmission errors of sun gear and planet gear  $j$

$e_{12}$  transmission errors of gear 1 and gear 2

$e_{34}$  transmission errors of gear 3 and gear 4

$\mathbf{F}_{in}$  vector of internal excitation forces

$\mathbf{F}_{ex}$  vector of external excitation forces

$i_s$  transmission ratio of the system.

$k_{rpi}$  meshing stiffness of ring gear and planet gear  $j$

$k_{spj}$  meshing stiffness of sun gear and planet gear  $j$

$k_{12}$  meshing stiffness of gear 1 and gear 2

$k_{34}$  meshing stiffness of gear 3 and gear 4

$k_{s1}$  torsional stiffness of connecting shafts between sun gear and gear 1

$k_{23}$  torsional stiffness of connecting shafts between gear 2 and gear 3

$\mathbf{K}$  stiffness matrix

$K_{\alpha q}$  load distribution factor of gear teeth at  $\mathbf{q}$

$k_q$  comprehensive meshing stiffness of tooth pair at  $\mathbf{q}$

$k_{q1}$  meshing stiffness of the tooth pair where  $\mathbf{q}$  is on

$k_{q2}$  meshing stiffness of the other tooth pair

$l$  turbulence scale parameter

$m$  module

$\mathbf{M}$  mass matrix

$n_t$  number of sampling points for a single tooth

$n_o$  number of sampling points in a vibration period

times of the  $i$  th short term wind speed model that appears in one year

$p$  order of AR Model

$P_{in}$  input power

$r_s$  base circle radius of sun gear

$r_1$	base circle radius of gear 1	$\Delta_{12}$	relative linear displacement between gear 1 and gear 2
$r_2$	base circle radius of gear 2	$\Delta_{34}$	relative linear displacement between gear 3 and gear 4 respectively
$r_3$	base circle radius of gear 3	$\Delta_{s1}$	relative torsional displacement between two ends of connecting shaft of sun gear and gear 1
$r_4$	base circle radius of gear 4	$\Delta_{23}$	relative torsional displacement between two ends of connecting shaft of gear 3 and gear 4
$t$	time	$\Delta$	displacement vector
$t_s$	time to start meshing	$\Delta t$	time step
$t_e$	time to end meshing	$\varepsilon$	contact ratio of the gear drive.
$T_{in}$	input torque	$\zeta_i$	modal damping ratio of the $i$ th order
$T_{out}$	output torque	$\eta_i$	natural coordinate of the $i$ th order
$T_m$	meshing period of the gear drive	$\kappa$	shape parameter of Weibull Distribution
$T_s$	sampling period	$\rho$	air density
$u_c$	linear displacement of planetary carrier on the tangential direction of base circle	$\zeta$	scale parameter of Weibull Distribution
$u_s$	linear displacement of sun gear on the tangential direction of base circle	$\sigma$	standard deviation
$u_{pj}$	linear displacement of planet gear $j$ on the tangential direction of base circle, $j = 1, 2, 3$	$\sigma_{qF}$	tooth root bending stress of $\mathbf{q}$
$u_l$	linear displacement of gear $l$ on the tangential direction of base circle, $l = 1, 2, 3, 4$	$\sigma_{aa}$	amplitude of asymmetrical cyclic stress
$V$	instantaneous wind speed	$\sigma_{ss}$	amplitude of symmetrical cyclic stress
$V_i$	short term wind speed of part $i$	$\sigma_m$	mean value of asymmetrical cyclic stress
$V_{ie}$	mean wind speed of part $i$	$\sigma_b$	tensile strength of the material
$\bar{V}$	mean wind speed	$\phi_p$	gear rotation angle when the meshing point moves from the initial meshing point to $\mathbf{p}$
$V'$	turbulent wind speed	$\psi$	autoregressive coefficient
$x$	$x$ direction	$\Phi^{(i)}$	eigenvector of the $i$ th order
$y$	$y$ direction	$\omega$	frequency
$Y_{Fq}$	tooth form factor	$\omega_c$	rotational speed of planet carrier
$Y_{Sq}$	stress correction factor	$\omega_s$	sampling frequency
$z$	$z$ direction	$\omega_{max}$	maximum natural frequency of the transmission system in different meshing positions
$z_g$	tooth number of the gear	$\omega_{di}$	damping natural frequency of the $i$ th order
<b>Greek symbols</b>		$\omega_g$	rotation speed of the gear
$\alpha_{sp}$	meshing angle of sun gear and planet gear		
$\alpha_{rp}$	meshing angle of ring gear and planet gear		
$\alpha_f$	radius of initial meshing point of the gear		
$\alpha_q$	pressure angle of $\mathbf{q}$		
$\gamma$	initial meshing phase, $0 < \gamma < 1$		
$\Delta_{rpi}$	relative linear displacement between ring gear and planet gear $j$		
$\Delta_{spi}$	relative linear displacement between sun gear and planet gear $j$		

## 風電齒輪傳動系統齒根彎曲應力之分佈特徵

吳陽 侯力 羅嵐  
四川大學機械工程學院

馬登秋  
遵義師範學院工學院

魏永峭  
蘭州理工大學機械工程學院

### 摘要

本文對風電齒輪傳動系統中齒輪的齒根彎曲應力分佈特徵進行了研究。為了得到更精確的結果，本文考慮了風速長期和短期的分佈特徵，考慮了單個輪齒的嚙合特徵和振動狀態。提出了系統計算風電齒輪傳動系統齒根彎曲應力的計算流程。基於香農定理和齒輪動力學提出了一種採樣方法，通過對齒輪相對位移歷程進行簡化以減少應力歷程計算的數據量從而提高計算效率。計算齒根應力時，單個輪齒被當作齒輪上的獨立單元進行處理，基於齒輪嚙合原理考慮了單個輪齒的嚙合過程。最後，基於本文方法，計算了太陽輪齒根彎曲應力的概率密度分佈曲線。探討了在兩個阻尼水準下，太陽輪彎曲應力概率分佈特徵相對於齒側間隙偏移量的變化規律。